Ozone sensitivity to varying greenhouse gases and ozone-depleting substances in CCMI simulations

Olaf Morgenstern[1], Hideharu Akiyoshi[2], Yousuke Yamashita[2,a], Douglas
E. Kinnison[3], Rolando R. Garcia[3], David A. Plummer[4], John Scinocca[5],
Guang Zeng[1], Eugene Rozanov[6,7], Andrea Stenke[7], Laura E. Revell[7,8],
Giovanni Pitari[9], Eva Mancini[9,10], Glauco Di Genova[10], Sandip S. Dhomse[11], and
Martyn P. Chipperfield[11]

[1]National Institute of Water and Atmospheric Research (NIWA), Wellington, New Zealand
[2]National Institute of Environmental Studies (NIES), Tsukuba, Japan
[3]National Center for Atmospheric Research (NCAR), Boulder, Colorado, USA
[4]Environment and Climate Change Canada, Montréal, Canada
[5]CCCMA, University of Victoria, Victoria, Canada
[6]Physikalisch-Meteorologisches Observatorium Davos – World Radiation Center, Davos,
Switzerland
[7]Institute for Atmospheric and Climate Science, ETH Zürich, Zürich, Switzerland
[8]Bodeker Scientific, Christchurch, New Zealand
[9]Dipartimento di Scienze Fisiche e Chimiche, Università dell'Aquila, L'Aquila, Italy
[10]CETEMPS, Università dell'Aquila, L'Aquila, Italy
[11]School of Earth and Environment, University of Leeds, Leeds, UK
[a]now at: Japan Agency for Marine-Earth Science and Technology (JAMSTEC), Yokohama, Japan

Correspondence to: Olaf Morgenstern (olaf.morgenstern@niwa.co.nz)

Abstract. Ozone fields simulated for the Chemistry-Climate Model Initiative (CCMI) will be used as forcing data in the 6th Coupled Model Intercomparison Project (CMIP6). Here we assess, using reference and sensitivity simulations produced for phase 1 of CCMI, the suitability of CCMI-1 model results for this process, investigating the degree of consistency amongst models regarding their responses to variations in individual forcings. We consider the influences of methane, nitrous oxide, a combination of chlorinated or brominated ozone-depleting substances (ODSs), and a combination of carbon dioxide and other greenhouse gases (GHGs). We find varying degrees of consistency in the models' responses in ozone to these individual forcings, including some considerable disagreement. In particular, the response of total-column ozone to these forcings is less consistent across the multi-model ensemble than profile comparisons. The likely cause of this is lower-stratospheric transport and dynamical responses exhibiting substantial inter-model differences. The findings imply that the ozone fields derived from CCMI-1 are subject to considerable uncertainties regarding the impacts of these anthropogenic forcings.

1 Introduction

The Chemistry-Climate Model Initiative (CCMI), in its first phase, has produced an unprecedented wealth of simulations by 20 chemistry-climate and chemistry-transport models (Eyring et al., 2013).

All of them comprise interactive chemistry schemes focussed on the simulation of stratospheric and/or tropospheric ozone, but there are significant differences in their formulations that affect chemistry as well as other aspects (Morgenstern et al., 2017). One purpose of CCMI is to inform

20 the upcoming 6th Coupled Model Intercomparison Project (CMIP6; Eyring et al., 2016), and particularly to provide pre-calculated ozone climatologies to those CMIP6 General Circulation Models (GCMs) that do not simulate ozone interactively. This is complicated by significant inter-model differences amongst the CCMI models as well as the fact that CMIP6 will explore a variety of Shared Socio-economic Pathways (SSPs; Riahi et al., 2016) that expand on the Representative Concentra-

25 tion Pathways (RCPs; Meinshausen et al., 2011) forming the basis of CMIP5 and the first phase of CCMI. Hence there is a requirement for a robust mechanism to turn the CCMI ozone fields into merged climatologies that are consistent with those SSPs. The feasibility of this processing step hinges upon the degree of consistency with which the CCMI models respond to variations in forcing fields; this is the topic of the present paper. More generally, the presence of targeted sensitivity

30 simulations in the CCMI ensemble allows us to study in detail the model responses to forcings by individual gases, which are of significant scientific interest irrespectively of applications in CMIP6. Here we only assess the model responses to long-lived gas forcings. Regarding short-lived climate agents, there are large inter-model differences in the representation of tropospheric ozone chemistry (Morgenstern et al., 2017) as well as spatially very heterogeneous emissions of ozone precursors.

35 Due to these additional complexities, comprehensively assessing the consistency of the simulation of tropospheric ozone in CCMI models needs to be the topic of a separate paper. Notwithstanding this, large-scale global climate and composition change can influence surface ozone through in-situ chemistry, long-range transport, stratosphere-troposphere exchange, changes in temperature and humidity, and radiative transfer.

40 We consider separately the influences of the following four different anthropogenic forcings on ozone (O_3): methane (CH_4), nitrous oxide (N_2O), ozone-depleting substances (ODSs, comprising chlorofluorocarbons, other organic chlorine compounds, methyl bromide, halons and other organic bromine compounds), grouped together as "equivalent chlorine" (Cl^{eq}), and a group of greenhouse gases (GHGs) comprising CO_2 and fluorinated compounds (hydrofluorocarbons, HFCs, perfluoro-

45 carbons, PFCs, and sulfur hexafluoride, SF_6) that do not act as ODSs. These gases are grouped together here as "CO_2-equivalent" (CO_2^e). All of these influences have been studied before (see below), but not all of them in a multi-model context. In all cases these forcings have both direct radiative (as GHGs) and chemical impacts. For the RCPs, the combined radiative impacts of GHGs can be summarized as warming the troposphere and cooling the stratosphere, with associated dy-

50 namical consequences, but the chemical impacts are more complicated and also induce secondary effects such as perturbations to stratospheric water vapour and ozone which themselves link to dynamics. This complexity opens up the potential for differences in model behaviour, the topic of this paper.

Several previous studies have investigated the linkages between CH_4 and O_3 (e.g., Stevenson
et al., 2000; Prather et al., 2001; Revell et al., 2012a; Morgenstern et al., 2013; Naik et al., 2013;
Voulgarakis et al., 2013). Generally, these studies have found that methane increases lead to ozone
increases in most of the lower and middle atmosphere which amplify the global warming associated
with methane. These increases are associated with a few different mechanisms, including methane's
role as an ozone precursor in the troposphere and a slow-down of chlorine-catalyzed ozone depletion
by $Cl + CH_4 \rightarrow HCl$. Since IPCC (2007), this link between CH_4 and O_3 has been accounted for
by stating an effective global warming potential for CH_4 that takes into account those chemical
feedbacks, also to due stratospheric water vapour production by methane oxidation. We will assess
here the consistency to which the methane-ozone link is simulated in CCMI models.

The impact of N_2O on O_3 is thought to be well understood (e.g., Portmann et al., 2012; Revell
et al., 2012b; Stolarski et al., 2015). N_2O is generally chemically inactive in the troposphere. In the
stratosphere it decays to form nitrogen oxides ($NO_x = NO + NO_2$) in a minor decay channel. NO_x
then participates in catalytic ozone depletion (Brasseur et al., 1999). It is the third most important
anthropogenic greenhouse gas after CO_2 and CH_4 (IPCC, 2007) and is now the leading ODS by
emissions (Ravishankara et al., 2009).

The impact of organic halogens on stratospheric ozone is likewise well understood (for a review
see Solomon, 1999). Essentially, these gases rise into the stratosphere where they release their halo-
gen atoms which then engage in ozone depletion. This is particularly pronounced in the polar regions
where chlorine is "activated" on polar stratospheric clouds, causing the Antarctic ozone hole to form
(Farman et al., 1985) and also causing usually less severe but highly variable ozone depletion in the
Arctic. This means their chemical impacts occur mostly in the "chlorine layer" around 40 km and in
the lower stratosphere over the poles (Brasseur et al., 1999). However, through dynamical feedbacks,
transport, and impacts on ultraviolet radiation such ozone depletion affects atmospheric composi-
tion throughout the troposphere and stratosphere (Madronich and Granier, 1992; Madronich, 1993;
Fuglestvedt et al., 1994, 1995; Morgenstern et al., 2013). Southern-Hemisphere climate change is
thought to have been dominated in recent decades by ozone depletion (for a review see Thompson
et al., 2011), but there is limited evidence for an effect of Arctic ozone depletion on the Northern-
Hemisphere circulation (Morgenstern et al., 2010). Under the Montreal Protocol, halogen-catalyzed
ozone depletion is anticipated to reverse (WMO, 2014); a recovery of the Antarctic ozone hole is
now unambiguously identified in observations (Solomon et al., 2016).

For analysis purposes, the ODSs are combined into a single index, equivalent chlorine (Cl^{eq}),
which is the sum of all chlorinated and brominated organic compounds as imposed at the Earth'
surface, weighted by the number of halogen atoms per molecule and multiplied by 60 for bromi-
nated compounds (Newman et al., 2007). Cl^{eq} excludes here dibromomethane (CH_2Br_2) and tri-
bromomethane ($CHBr_3$) which significantly impact stratospheric ozone levels (Oman et al., 2016).
They are imposed as invariant constants (Morgenstern et al., 2017) and hence are thought not to

contribute to any trends. Cl^{eq} is shifted by 4 years relative to the A1 scenario (WMO, 2014) to better represent the time it takes for the turn-around in halogens caused by the implementation of the Montreal Protocol to propagate to middle and high latitudes of the stratosphere.

Finally, the gases grouped as CO_2^e, comprising CO_2, hydrogenated fluorocarbons (HFCs), perfluorocarbons (PFCs), and SF_6, are not thought to have a significant direct chemical impact on ozone, but as greenhouse gases have substantial impacts on temperature, humidity, and circulation, which in turn affect ozone (IPCC, 2013). Under the scenario assumed here, the fluorinated gases do not contribute much to global warming, i.e. the reference simulations described below assume moderate emissions of them (Meinshausen et al., 2011). CO_2, the leading gas in this group, undergoes roughly a doubling between 1960 and 2100 in this scenario. Morgenstern et al. (2017) show graphs of all the long-lived forcings used here. While these gases, for the purposes of this paper, are combined into one measure (CO_2^e), their actual treatment varies by model, with some models considering or not considering certain minor GHGs in their radiation schemes (Morgenstern et al., 2017). Some others use lumping which in itself has certain limitations. For example, increases in CO_2 are cooling the stratosphere whereas increases in HFCs would warm it (Hurwitz et al., 2015), meaning that CO_2 is not a perfect analogue to HFCs in our model simulations. However simulations that would target separately the impacts of HFCs do not exist in the CCMI ensemble.

In this paper, we assess the degree of consistency found across the CCMI ensemble w.r.t. the impact of these forcings on ozone. We will do so by using sensitivity simulations performed for CCMI. One limitation of this approach is that it does not account for nonlinear interactions between the forcings (e.g., stratospheric cooling caused by CO_2 slows down gas-phase ozone depletion Portmann et al., 2012; Dhomse et al., 2016). We will address this further in the final section.

2 Models and data

2.1 Experiments used in this paper

Here we use simulations performed under the following experiments as requested for CCMI. The simulations generally cover 1960-2100 unless stated otherwise (Eyring et al., 2013; Morgenstern et al., 2017):

- REF-C2: In this experiment, GHGs, CH_4 and N_2O follow the RCP 6.0 scenario (Meinshausen et al., 2011), and ODSs follow the A1 scenario of WMO (2014).

- SEN-C2-fCH4: Same as REF-C2, except CH_4 is held fixed at its 1960 value (Hegglin et al., 2016).

- SEN-C2-fN2O: Same as REF-C2, except N_2O is held fixed at its 1960 value (Hegglin et al., 2016).

– SEN-C2-fODS: Same as REF-C2, except all chlorinated and brominated ODSs are held at
their 1960 values.

– SEN-C2-fGHG: Same as REF-C2, except CO_2, CH_4, N_2O, and other non-ozone depleting
GHGs are held at their 1960 values.

– SEN-C2-RCP85: Same as REF-C2, except the GHGs, CH_4 and N_2O follow the RCP 8.5
scenario (Meinshausen et al., 2011). These simulations cover 2000-2100.

SEN-C2-fCH4, SEN-C2-fN2O, SEN-C2-fODS, and SEN-C2-fGHG simulations address the sensitivities to individual forcings, whereas the SEN-C2-RCP85 experiment assesses the impacts of the variant RCP 8.5 scenario that can be seen as a simultaneous variation of multiple forcings relative to the reference simulation. We use RCP 8.5 here because it is characterized by the largest anthropogenic forcings. In particular, CH_4 growth is much more pronounced than in REF-C2 / RCP 6.0 (Meinshausen et al., 2011).

2.2 Models used in the paper

We use CCMI model simulations for which ozone has been archived for REF-C2 and any of the other 4 sensitivity experiments. For the assessment of the influences of GHGs, we require simulations covering REF-C2, SEN-C2-fGHG, SEN-C2-fCH4, and SEN-C2-fN2O (see below). Table 1 lists the models and the number of simulations used for the sensitivity analysis in section 3. UMSLIMCAT

Table 1: Models used in this paper, with associated ensemble sizes of CCMI simulations conducted.

Model and reference	REF-C2	fCH4	fN2O	fODS	fGHG	RCP85
CCSRNIES-MIROC3.2 (Akiyoshi et al., 2016)	2	1	1	1	1	1
CESM1 WACCM (Garcia et al., 2017)	3	1	1	3	3	3
CMAM (Scinocca et al., 2008)	1	1	1	1	1	1
NIWA-UKCA (Morgenstern et al., 2009)	5	1	1	2	3	
SOCOL3 (Stenke et al., 2013)	1	1	1			
ULAQ-CCM (Pitari et al., 2014)	2	2	2	1	1	1
UMSLIMCAT (Tian and Chipperfield, 2005)	1				1	

also conducted the SEN-C2-fGHG and SEN-C2-RCP85 experiments, but because of the missing SEN-C2-fCH4 and and SEN-C2-fN2O simulations, these will not be considered here.

These seven models are described by Morgenstern et al. (2017) and references therein. Except for NIWA-UKCA, they all use hybrid-pressure (or actual pressure, in the case of ULAQ-CCM) as their vertical coordinate. NIWA-UKCA uses hybrid-height levels. Except for UMSLIMCAT, we start out with zonally resolved ozone on model levels for this analysis. UMSLIMCAT data come on 31 pressure levels extending to 0.1 hPa. The CCSRNIES-MIROC3.2 simulations were conducted

on two different computers (REF-C2 (1), SEN-C2-fODS, SEN-C2-fGHG, and SEN-C2-RCP85 on

an NEC SX9 machine, and REF-C2 (2), SEN-C2-fCH4, and SEN-C2-fN2O on an NEC SX-ACE).

150   This resulted in some differences between the two REF-C2 simulations. We have therefore repeated

all calculations detailed below now assuming that the CCSRNIES-MIROC3.2 simulations represent

two different models. The results are essentially unchanged versus what is presented here. Hence for

the purposes of this paper, CCSRNIES-MIROC3.2 is treated as one model.

UMSLIMCAT and CCSRNIES-MIROC3.2 have prescribed or only partially interactive tropo-

155   spheric composition (Morgenstern et al., 2017) and are hence ignored in the analysis of tropospheric

features such as the response of total-column ozone to methane changes, and in any assessments of

surface ozone.

2.2.1   Method of analysis

We form zonally averaged ozone on model levels as represented by the CCMI models. Next, we

160   perform a first-order Taylor expansion around the reference case defined by REF-C2. This means

$$\Delta O_3 = a\Delta CH_4 + b\Delta N_2O + c\Delta Cl^{eq} + d\Delta CO_2^e + \epsilon. \tag{1}$$

Here, ΔO_3 is the difference in ozone between two different scenarios, ΔCH_4 and ΔN_2O are the

differences in methane and nitrous oxide, respectively, and ΔCO_2^e and ΔCl^{eq} are the differences in

carbon dioxide-equivalent and equivalent chlorine as defined above.

165   a, b, c, and d are determined using least-squares linear regression. Functions of latitude, level, and

month of the year, they minimize the residual ϵ. For example, to determine a we use the difference

in the zonal-mean ozone fields from REF-C2 and SEN-C2-fCH4:

$$\Delta O_3 = a\Delta CH_4 + \epsilon \tag{2}$$

and determine a by regressing, at every latitude, model level, and month, the 140- or 141-year time-

170   series of ΔO_3 against the same-length timeseries of ΔCH_4, which is the global-mean methane

mixing ratio as defined under RCP 6.0 minus its value in 1960. Equivalent analyses yield b, using

REF-C2 and SEN-C2-fN2O, and c, using REF-C2 and SEN-C2-fODS. The SEN-C2-fGHG simula-

tion keeps all GHGs including CH_4 and N_2O, but excluding ODSs, fixed at their 1960s levels. To

account for the effects of fixing CH_4 and N_2O, we form a modified ozone field

175    $$O_3' = O_3(SEN\text{-}C2\text{-}fGHG) + a\Delta CH_4 + b\Delta N_2O \tag{3}$$

which is derived from the ozone field produced by the SEN-C2-fGHG experiment, O_3(SEN-C2-

fGHG), but with the impacts of differences in CH_4 and N_2O added. We then use the difference

$\Delta O_3 = O_3(REF\text{-}C2) - O_3'$ in our regression analysis as before to determine d.

In this formulation, the forcings (except Cl^{eq}) are as imposed at the surface, so transport-related

180   delays are not accounted for. Such delays primarily result from the time it takes for a long-lived

tracer, emitted at the surface, to reach the stratosphere. For the forcings other than Cl^{eq} this is not critical as their tendencies are only slowly varying, i.e. they do not display the sharp turn-around characterizing Cl^{eq}.

In cases where multiple simulation are available for a given scenario and model, the ensemble
185 average is used in the analysis.

3 Results

3.1 Sensitivity of ozone to methane

Figure 1 shows the sensitivity of zonal-mean ozone with respect to changes in CH_4 (i.e., a) as derived from the REF-C2 and SEN-C2-fCH4 experiments. Six models have conducted both experiments. In
190 the middle and upper stratosphere, there is a region where CH_4 increases cause ozone increases by around 10% to 40% of the increase of the prescribed surface methane mixing ratio. This may be because of the $CH_4 + Cl \rightarrow HCl$ reaction which returns chlorine to HCl not involved in ozone depletion. Higher up, above the stratopause at approximately 1 hPa, methane increases cause ozone to decline, due to increases in HO_x related ozone depletion under increasing methane (Morgen-
195 stern et al., 2013, and references therein). There is considerable uncertainty regarding the size of this feedback. CCSRNIES-MIROC3.2 and CMAM simulate extensive regions where seasonally or in all seasons the ozone decline exceeds 10% of the methane difference, whereas in ULAQ-CCM this effect is generally smaller than 5%. In the tropical upper-troposphere/lower stratosphere (UTLS) region, most of the models simulate a negative feedback, i.e. methane increases cause a decrease in
200 ozone, but the size and spatial extent of this effect is highly uncertain, with NIWA-UKCA producing ozone decreases of 10-20% of the methane difference. In the other models, there are some decreases, but they are insignificant in parts of the latitude-pressure domain at the 95% confidence level, peaking at less than 10% of the applied methane increase in CCSRNIES-MIROC3.2, CESM1-WACCM, and SOCOL3.
205 The equivalent analysis for zonal-mean total-column ozone (TCO; figure 2) indicates that indeed CH_4 increases generally cause a TCO increase everywhere (apart from over the South Pole in the ULAQ-CCM). In the tropics, the increase is smaller in CESM1-WACCM and NIWA-UKCA than in the other models, which is in agreement with the relatively pronounced negative feedback in the UTLS region found above for both models, which for the TCO offsets the ozone increases higher
210 up. CESM1-WACCM and NIWA-UKCA also have larger TCO increases during winter/spring over the Arctic than the other models.

Figure 3 shows the zonal-mean sensitivity a at the surface as a function of month of the year and latitude. The five models exhibit some common features but also some considerable qualitative and quantitative differences in their responses to methane increases. Commonalities include that methane
215 increases cause statistically significant ozone increases everywhere. This is as expected, given the

role of methane as an ozone precursor. In all five models, the increase maximizes in northern mid-latitudes, but the seasonality of this feature varies by model. There is a secondary maximum in the Southern-Hemisphere winter. In three of the models (CESM1-WACCM, CMAM, NIWA-UKCA) the response minimizes at the South Pole during summer. Both SOCOL3 and ULAQ-CCM have a very small seasonal cycle of this feature over the South Pole. In CESM1-WACCM, there are three distinct minima in the response of ozone to methane increases, located at around $65°$S in January, in the tropics throughout the year, and in the Arctic from June to September.

Differences that divide these results are partly about magnitude of the signal (NIWA-UKCA simulations show the smallest sensitivity of surface ozone to methane increases, followed in order by CESM1-WACCM, CMAM, SOCOL3, and ULAQ-CCM). Also details of the annual cycle differ. For example, CESM1-WACCM, CMAM, and SOCOL3 produce a minimum over the Arctic in summer; there is no sign of this occurring in NIWA-UKCA and ULAQ-CCM. The relatively strong response of SOCOL3 surface ozone to CH_4 increases may be related to a general overestimation of tropospheric ozone in the Northern Hemisphere by that model (Revell et al., 2015).

3.2 Sensitivity of ozone to nitrous oxide

Figure 4 shows the sensitivity to zonal-mean N_2O changes (*b*) as derived from the REF-C2 and SEN-C2-fN2O experiments. The same six models as discussed in section 3.1 also conducted SEN-C2-fN2O. The sensitivity to N_2O increases is more coherently simulated by the models than that to CH_4, with the models largely agreeing on the main features. In the upper stratosphere, N_2O increases cause a decrease in O_3 of about 5 to 9 times the increase in N_2O, peaking in all seasons in the tropics. Above 1 hPa, there is disagreement on the sign of the ozone response, with CCSRNIES-MIROC3.2 and ULAQ-CCM producing mostly increasing ozone for increases in N_2O, whereas CESM1-WACCM, NIWA-UKCA, and SOCOL3 produce partly insignificant decreases in most regions, but also, in the case of CESM1-WACCM, some increases. In CMAM, the co-variance of ozone with surface N_2O appears to be insignificant almost everywhere. In the lower stratosphere, all models produce some increases in ozone for increases in N_2O. This may be the result of a self-healing process, whereby ozone depletion higher up caused by increased N_2O allows more UV light to penetrate to this level, producing more ozone there. The meridional extent and magnitude of the ozone increase vary by model. In CESM1-WACCM, NIWA-UKCA, and SOCOL3 the ozone increase covers the whole latitude range, whereas in CMAM and ULAQ-CCM the belt does not consistently extend to the poles. In CCSRNIES-MIROC3.2, this feature is weaker than in the other models and partially insignificant.

Like for methane, the response of TCO to N_2O changes is highly model-dependent (figure 5). Best agreement across the six-models ensemble is achieved in the tropics, where all models find decreases in TCO for increases in N_2O ranging around -0.075 to -0.05 DU/ppbv in CCSRNIES-MIROC3.2 to roughly -0.03 Dobson Units (DU)/ppbv in NIWA-UKCA, SOCOL3, and ULAQ-

CCM. In the northern extratropics, several of the models agree on the phasing of the annual cycle, with TCO decreases maximizing in late winter/spring and minimizing in late summer. In the southern extratropics, a similar seasonality is evident. SOCOL3 exhibits significant increases under

255   N_2O increases over Antarctica in spring, and NIWA-UKCA has relatively weak decreases and some seasonal increases under N2O increases, particularly in the Arctic in summer. Both are associated with anomalously large increases in the lower stratosphere evident in figure 4, suggesting that dynamical/chemical feedbacks in the lower stratosphere overcompensate for the additional chemical depletion that all models show in the middle stratosphere. Even for this forcing, to which the models

260   simulate a generally consistent response in the middle stratosphere, the extratropical TCO response remains quantitatively uncertain.

Figure 6 shows b evaluated at the surface. Generally, as N_2O is chemically inert in the troposphere, four of the models show large areas of insignificant covariance between N_2O and surface O_3, particularly in the extratropics. As for significant features, the same four models agree on a decrease

265   in ozone in the tropics, also extending into northern midlatitudes in summer, of -0.002 to -0.004 times the increase in N_2O, and an increase of ozone by roughly 0.002 times the increase in N_2O in southern mid-latitudes during winter. In CESM1-WACCM, this feature in more pronounced, covering much of the southern extratropics, and is significant year-round. The feature is insignificant in CMAM. ULAQ-CCM, by contrast, shows significant increases in surface ozone almost everywhere

270   for an increase in N_2O, peaking in northern midlatitudes, i.e. it is in disagreement with the other models regarding both magnitude and shape of the annual cycle of b.

3.3   Sensitivity of ozone to equivalent chlorine

Figure 7 shows the sensitivity of zonal-mean ozone to changes in Cl^{eq} (section 1), as derived from the REF-C2 and SEN-C2-fODS experiments. Six models have conducted both of these experiments. In

275   the upper stratosphere, there is a consistent decrease in ozone by up to -700 times the Cl^{eq} increase. This is consistently simulated by all models, and is the consequence of global halogen-catalyzed ozone depletion maximizing at around 40 km. Higher up, above approximately 1 hPa, the models simulate mostly a decrease of 0 to 50 times the EESC increase. There also are consistent decreases in ozone in the lower stratosphere / tropopause region of the southern high latitudes during spring

280   and summer, associated with the ozone hole. In January, in what is likely a dynamical feedback, there is an increase in ozone (for an increase in ODSs) between about 50 and 10 hPa / 25-32 km. In CCSRNIES-MIROC3.2, CESM1-WACCM, CMAM, and UMSLIMCAT, Antarctic October polar ozone depletion occupies the entire lower stratosphere, between $\sim$ 200 and 10 hPa, with ozone loss reaching 1000 times the difference in Cl^{eq}.

285   Regarding the response of the TCO to Cl^{eq} changes, the models uniformly exhibit decreases in TCO for an increase in Cl^{eq} (figure 8). In the tropics, there is reasonable agreement regarding the size of the effect. In the extratropics, there is some quantitative disagreement. Best agreement is found

over the Antarctic in spring, where the models in October agree to within ± 10 DU/ppbv(Cl$^{\text{eq}}$) with each other. This agreement may be the result of a long-term focus on this region for the impact of ozone depletion. By contrast, in the Arctic significant quantitative differences are apparent regarding this effect.

As for surface ozone, there is little agreement as to the impacts of this stratospheric ozone depletion (figure 9). In NIWA-UKCA, there is a widespread decrease in surface ozone associated with stratospheric ozone depletion, with maxima in both mid-latitude regions during autumn. The southern one is larger, reaching the size of the difference in Cl$^{\text{eq}}$. The near-symmetry between the two hemispheres is in agreement with the pronouced Arctic ozone depletion produced by NIWA-UKCA (figure 7). CESM1-WACCM and CMAM produce a southern-hemisphere maximum of similar magnitude, but CMAM produces a secondary maximum over the South Pole in spring, and the response in the Northern Hemisphere in both models is much smaller than in NIWA-UKCA. ULAQ-CCM disagrees with the other three models in that in the Northern Hemisphere and the tropics, ozone mostly increases under increases of Cl$^{\text{eq}}$. In the southern extratropics, this model largely produces decreases but the effect maximizes in austral summer, i.e. the seasonality disagrees with the other three models.

It is noteworthy that three of the four models display their peak response of surface ozone to stratospheric ozone depletion in austral autumn, approximately 6 months after the onset of the Antarctic ozone hole.

3.4 Sensitivity of ozone to GHGs

Here we assess the sensitivity of ozone to increases in CO$_2^{\text{e}}$ (section 1). Increases in CO$_2^{\text{e}}$ cause increases of ozone peaking between roughly 10 and 1 hPa; these increases are of similar magnitude in all models (figure 10). They also cause decreases in ozone in the tropical and subtropical lower stratosphere; again there is largely agreement about the magnitude of this effect. Both the decrease and the increase may be aspects of an upward displacement and associated acceleration of the Brewer-Dobson Circulation (Butchart, 2014; Oberländer-Hayn et al., 2016). Also stratospheric cooling, through its impact on ozone-depleting chemical cycles, leads to an increase in stratospheric ozone. In the mesosphere, there is quantitative disagreement regarding the impact of increases in CO$_2^{\text{e}}$. CESM1-WACCM, CMAM, and ULAQ-CCM exhibit mostly or generally increases, whereas in NIWA-UKCA and CCSRNIES-MIROC3.2 such increases cause ozone to decline. The models also generally agree on a region of ozone decrease in the tropical and subtropical lower stratosphere which reaches -0.5×10^{-3} to -2×10^{-3} times the increase in the CO$_2^{\text{e}}$ VMR.

Regarding the TCO response to CO$_2^{\text{e}}$ increases (figure 11), there is reasonable agreement across the models except CESM1-WACCM as to the general impact, namely a decrease in TCO in the tropics, maximizing in boreal winter/spring, and increases in the extratropics (Eyring et al., 2010). In CESM1-WACCM, the relatively small increases in O$_3$ in the tropical lower stratosphere (figure

10) are outweighed by decreases in the troposphere and middle/upper stratosphere, meaning this
model does not exhibit tropical TCO decreases under increasing CO_2^e, unlike the other models.
Similar cancellations of ozone trends at different altitudes also happen in the other models, with
tropical TCO trends constituting a small residual. Therefore the fact that CESM1-WACCM does
not produce negative trends there has to be seen as a quantitative not a qualitative disagreement.
Increases in the Northern Hemisphere during boreal winter and spring are consistent across the five
models; they exceed those in the South. There is no agreement regarding the seasonality of the effect
in the southern extratropics. CMAM produces some significant decreases in TCO in response to
CO_2^e increases over the South Pole in austral spring; the other models do not simulate this feature.

As for surface ozone, CMAM, NIWA-UKCA, and ULAQ-CCM mostly produce decreases of sur-
face ozone for an increase in CO_2^e, but also some increases at northern high latitudes during autumn,
winter, and spring (figure 12). CESM1-WACCM produces smaller changes in ozone under climate
change; they are negative (0 to -5 ppbv/ppmv) in the tropics and in the SH during summer and posi-
tive (0 to 5 ppbv/ppmv) at other times and seasons. In ULAQ-CCM, this increase is restricted to late
winter and spring. While the models agree about decreases in ozone in the tropics and mid-latitudes,
there is disagreement about the magnitude, with decreases in NIWA-UKCA smaller than in the other
models. CESM1-WACCM and NIWA-UKCA simulate significant ozone decreases over the Arctic in
summer. This may be the result of reductions of sea ice cover and associated decreased tropospheric
ozone formation in an ice-albedo feedback on photochemistry (Voulgarakis et al., 2009).

4   Linearity of the ozone response to greenhouse gas forcing

Based on the previous section, we calculate, assuming linear scaling and ignoring non-linear cou-
pling (Portmann et al., 2012; Dhomse et al., 2016), the ozone fields that would result from alternative
GHG scenarios other than the RCP 6.0 forcing used in REF-C2. For the moderate-emissions scenar-
ios RCP 2.6 and 4.5, this can be seen as a consistency test. For the more extreme RCP 8.5, where
forcings are partially outside the range spanned by RCP 6.0 / REF-C2 and the total ozone abundance
is larger than in REF-C2, this exercise will help highlight nonlinear couplings between the forcings.
The scaling is possible for those models that have produced the REF-C2, SEN-C2-fGHG, SEN-C2-
fN2O, and SEN-C2-fCH4 simulations. We produce scaled ozone fields for CCSRNIES-MIROC3.2,
CESM1-WACCM, CMAM, and ULAQ-CCM (NIWA-UKCA did not produce any SEN-C2-RCP
simulations needed for comparison here). For the more moderate RCPs 2.6 and 4.5, the ozone fields
resulting from such scaling in the zonal mean relatively accurately match those simulated by the
three models. Significant relative differences occur in the troposphere, where the scaling method is
not applicable (see above) and in the UTLS region, where changes in the tropopause height con-
stitute a non-linear feedback not well captured by simple scaling of the ozone fields (supplement,
figures S1 and S2). Larger differences, and generally of opposite sign relative to RCP2.6 and RCP

4.5 occur for RCP 8.5. Scaling generally overestimates middle- and upper-stratospheric ozone by

360   10 to 30%, underestimates mesospheric ozone, and also produces errors in the UTLS region (figure 13). Three of the models (CCSRNIES-MOIROC3.2, CESM1-WACCM, and CMAM) mostly agree on the general features of this diagnostic, whereas the ULAQ-CCM produces somewhat larger differences between simulated and scaled ozone fields which also differ in sign or shape in the mesosphere and troposphere.

365 **5 Conclusions**

We have analysed the sensitivities of ozone to changes in CH_4, N_2O, halogenated ODSs, and a combination of CO_2 and other greenhouse gases in seven CCMI models. In all cases we find some qualitative and quantitative agreement, mainly about the impacts in the middle stratosphere, but also considerable disagreements in other regions, particularly the troposphere, the UTLS region, and the

370   mesosphere. The middle-stratospheric impact of CH_4 increases is largely consistently simulated by the six models studied here, but significant differences occur in the lower stratosphere, the troposphere, and in the total-column impacts of increasing CH_4. The impacts on ozone of increasing N_2O are relatively consistently simulated, in particular regarding decreases in the middle stratosphere and increases in the lower stratosphere. Also three of the models agree to some extent on the relatively

375   small impact on surface ozone. However, as with CH_4, quantitative differences in the sensitivity of lower-stratospheric ozone to increases of N_2O mean that the response of the TCO to N_2O increases remains uncertain. The impact of changing ODSs on stratospheric ozone is well simulated, with some general agreement regarding the middle-stratospheric response and also the impact on polar ozone. There remain quantitative differences regarding the impact on the TCO, globally, and particu-

380   larly regarding the impact of stratospheric ozone depletion on surface ozone. Lastly, we have studied the effect of a combination of CO_2 and other GHGs on ozone. Essentially, global warming causes ozone in the middle stratosphere to increase and in the low-latitude lower stratosphere to decrease. The TCO impacts are relatively consistently simulated, but the response of surface ozone to global warming remains highly uncertain, with the four CCMI models suitable for this analysis disagree-

385   ing on major aspects of the impact. They exhibit larger differences regarding the impact of global warming on surface ozone than were found in a recent study using a different ensemble (Young et al., 2013). This may reflect uncertainties related to stratosphere-troposphere coupling that were suppressed in the large subset of the models examined by Young et al. (2013) which used prescribed stratospheric ozone. This may thus be an example of additional model complexity causing increased

390   divergence of results (Morgenstern et al., 2017).

In essence, it appears that mid- and upper-stratospheric impacts of the four gaseous anthropogenic forcings are relatively consistently simulated by the subset of CCMI models studied here, but lower-stratospheric, tropospheric, and mesospheric impacts often are not. The total-column response is

affected by dynamical feedbacks which are not consistent in the CCMI model ensemble. These
395 inconsistencies in the CCMI ensemble need to be considered and may have consequences for the
fidelity of any merged ozone climatologies produced from the CCMI results.

It is possible that the results presented here are subject to a sampling bias in the sense that they
require a relatively large number of sensitivity simulations to be available, which some more ex-
pensive, higher-resolution models in the CCMI ensemble have not performed. It is regrettable that
400 even though the CCMI ensemble nominally comprises 20 models (Morgenstern et al., 2017), only
seven models have been considered here, and of these, some are unsuitable for certain diagnoses,
e.g. because tropospheric composition is prescribed or because required simulations or diagnostics
do not exist. Nonetheless, the results point to the need to better characterize quantitatively the lower-
stratospheric climate-ozone feedbacks that are the likely cause for the discrepancies found here. The
405 impact of methane on ozone occurs significantly in the troposphere. Here differences in formulation
and sophistication of tropospheric chemistry also impact the models' responses to methane changes.
Such differences may also play into the responses to the other forcings, although the surface ozone
responses to N_2O increases are surprisingly consistent across most of the models, despite such dif-
ferences in formulation.

6 Availability of simulations

410

The ozone fields as used here are mostly as downloaded from the Centre for Environmental Data
Analysis (CEDA; ftp://ftp.ceda.ac.uk). CESM1-WACCM data have been downloaded from http:
//www.earthsystemgrid.org. For instructions for access to both archives see http://blogs.reading.ac.
uk/ccmi/badc-data-access. UMSLIMCAT data have been downloaded from http://homepages.see.
415 leeds.ac.uk/~fbsssdh/updated_ccmi.

Acknowledgements. We thank the Centre for Environmental Data Analysis (CEDA) for hosting the CCMI data
archive. We acknowledge the modelling groups for making their simulations available for this analysis, and the
joint WCRP SPARC/IGAC Chemistry-Climate Model Initiative (CCMI) for organizing and coordinating this
model data analysis activity. We acknowledge the UK Met Office for use of the MetUM. This research was
420 supported by the NZ Government's Strategic Science Investment Fund (SSIF) through the NIWA programme
CACV. OM acknowledges funding by the New Zealand Royal Society Marsden Fund (grant 12-NIW-006) and
by the Deep South National Science Challenge (http://www.deepsouthchallenge.co.nz). The authors wish to
acknowledge the contribution of NeSI high-performance computing facilities to the results of this research.
New Zealand's national facilities are provided by the New Zealand eScience Infrastructure (NeSI) and funded
425 jointly by NeSI's collaborator institutions and through the Ministry of Business, Innovation & Employment's
Research Infrastructure programme (https://www.nesi.org.nz). WACCM is a component of NCAR's Commu-
nity Earth System Model (CESM), which is supported by the National Science Foundation (NSF). Computing
resources (ark:/85065/d7wd3xhc) were provided by the Climate Simulation Laboratory at NCAR's Computa-

tional and Information Systems Laboratory, sponsored by the National Science Foundation and other agencies.

430   The SOCOL team acknowledges support from the Swiss National Science Foundation under grant agreement
      CRSII2_147659 (FUPSOL II). CCSRNIES's research was supported by the Environment Research and Tech-
      nology Development Fund (2-1303 and 2-1709) of the Ministry of the Environment, Japan, and computations
      were performed on NEC-SX9/A(ECO) and NEC SX-ACE computers at the CGER, NIES.

References

435   Akiyoshi, H., Nakamura, T., Miyasaka, T., Shiotani, M., and Suzuki, M.: A nudged chemistry-climate model
       simulation of chemical constituent distribution at northern high-latitude stratosphere observed by SMILES
       and MLS during the 2009/2010 stratospheric sudden warming, J. Geophys. Res. Atmos., 121, 1361–1380,
       doi:10.1002/2015JD023334, 2016.

       Brasseur, G. P., Orlando, J. J., and Tyndall, G. S., eds.: Atmospheric Chemistry and Global Change, Oxford

440   University Press, Oxford, United Kingdom, and New York, NY, USA, 1999.

       Butchart, N.: The Brewer-Dobson circulation, Rev. Geophys., 52, 157–184, doi:10.1002/2013RG000448, 2014.

       Dhomse, S. S., Chipperfield, M. P., Damadeo, R. P., Zawodny, J. M., Ball, W. T., Feng, W., Hossaini, R., Mann,
       G. W., and Haigh, J. D.: On the ambiguous nature of the 11 year solar cycle signal in upper stratospheric
       ozone, Geophys. Res. Lett., 43, 7241–7249, doi:10.1002/2016GL069958, 2016.

445   Eyring, V., Cionni, I., Bodeker, G. E., Charlton-Perez, A. J., Kinnison, D. E., Scinocca, J. F., Waugh, D. W.,
       Akiyoshi, H., Bekki, S., Chipperfield, M. P., Dameris, M., Dhomse, S., Frith, S. M., Garny, H., Gettelman,
       A., Kubin, A., Langematz, U., Mancini, E., Marchand, M., Nakamura, T., Oman, L. D., Pawson, S., Pitari,
       G., Plummer, D. A., Rozanov, E., Shepherd, T. G., Shibata, K., Tian, W., Braesicke, P., Hardiman, S. C.,
       Lamarque, J. F., Morgenstern, O., Pyle, J. A., Smale, D., and Yamashita, Y.: Multi-model assessment of

450   stratospheric ozone return dates and ozone recovery in CCMVal-2 models, Atmos. Chem. Phys., 10, 9451–
       9472, doi:10.5194/acp-10-9451-2010, 2010.

       Eyring, V., Lamarque, J.-F., Hess, P., Arfeuille, F., Bowman, K., Chipperfield, M. P., Duncan, B., Fiore, A.,
       Gettelman, A., Giorgetta, M. A., Granier, C., Hegglin, M. I., Kinnison, D., Kunze, M., Langematz, U.,
       Luo, B. P., Martin, R., Matthes, K., Newman, P. A., Peter, T., Robock, A., Ryerson, T., Saiz-Lopez, A.,

455   Salawitch, R., Schultz, M., Shepherd, T. G., Shindell, D., Staehelin, J., Tegtmeier, S., Thomason, L., Tilmes,
       S., Vernier, J.-P., Waugh, D. W., and Young, P. J.: Overview of IGAC/SPARC Chemistry-Climate Model
       Initiative (CCMI) community simulations in support of upcoming ozone and climate assessments, SPARC
       Newsletter, 40, 48–66, 2013.

       Eyring, V., Bony, S., Meehl, G. A., Senior, C. A., Stevens, B., Stouffer, R. J., and Taylor, K. E.: Overview of

460   the Coupled Model Intercomparison Project Phase 6 (CMIP6) experimental design and organization, Geosci.
       Model Dev., 9, 1937–1958, doi:10.5194/gmd-9-1937-2016, 2016.

       Farman, J. C., Gardiner, B. G., and Shanklin, J. D.: Large losses of total ozone in Antarctica reveal seasonal
       ClO_x/NO_x interaction, Nature, 315, 207–210, doi:10.1038/315207a0, 1985.

       Fuglestvedt, J. S., Jonson, J. E., and Isaksen, I. S. A.: Effects of reductions in stratospheric ozone on tropospheric

465   chemistry through changes in photolysis rates, Tellus, 46B, 172–192, 1994.

       Fuglestvedt, J. S., Jonson, J. E., Wang, W.-C., and Isaksen, I. S. A.: Responses in tropospheric chemistry to
       changes in UV fluxes, temperatures and water vapour densities, in: Atmospheric Ozone as a Climate Gas:
       General Circulation Model Simulations, edited by Wang, W.-C. and Isaksen, I. S. A., pp. 145–162, Springer
       Verlag, Berlin, Heidelberg, doi:10.1007/978-3-642-79869-6_10, 1995.

470   Garcia, R. R., Smith, A. K., Kinnison, D. E., de la Cámara, A., and Murphy, D.: Modifications of the gravity
       wave parameterization in the Whole Atmosphere Community Climate Model: Motivation and results, J.
       Atmos. Sci., pp. 275–291, doi:10.1175/JAS-D-16-0104.1, 2017.

Hegglin, M. I., Lamarque, J.-F., Duncan, B., Eyring, V., Gettelman, A., Hess, P., Myhre, G., Nagashima, T., Plummer, D., Ryerson, T., Shepherd, T., and Waugh, D.: Report on the IGAC/SPARC Chemistry-Climate

475   Model Initiative (CCMI) 2015 science workshop, SPARC Newsletter, 46, 37–42, 2016.

Hurwitz, M. M., Fleming, E. L., Newman, P. A., Li, F., Mlawer, E., Cady-Pereira, K., and Bailey, R.: Ozone depletion by hydrofluorocarbons, Geophys. Res. Lett., 42, 8686–8692, doi:10.1002/2015GL065856, 2015.

IPCC: Climate Change 2007: The Physical Science Basis. Contribution of Working Group I to the Fourth Assessment Report of the Intergovernmental Panel on Climate Change, Solomon, S., Qin, D., Manning,

480   M., Chen, Z., Marquis, M., Averyt, K. B., Tignor, M. and Miller, H. L. (eds.), Cambridge University Press, Cambridge, United Kingdom and New York, NY, USA, 2007.

IPCC: Climate Change 2013: The Physical Science Basis. Contribution of Working Group I to the Fifth Assessment Report of the Intergovernmental Panel on Climate Change, T. F. Stocker, D. Qin, G.-K. Plattner, M. Tignor, S. K. Allen, J. Boschung, A. Nauels, Y. Xia, V. Bex, and P. M. Midgley (eds.), Cambridge University

485   Press, 2013.

Madronich, S.: Tropospheric photochemistry and its response to UV changes, in: The role of the stratosphere in global change, edited by Chanin, M.-L., vol. 18 of *NATO-ASI Series*, pp. 437–461, Springer Verlag, Amsterdam, Netherlands, 1993.

Madronich, S. and Granier, C.: Impact of recent total ozone changes on tropospheric ozone photodissociation,

490   hydroxyl radicals, and methane trends, Geophys. Res. Lett., 19, 465–467, 1992.

Meinshausen, M., Smith, S. J., Calvin, K. V., Daniel, J. S., Kainuma, M. L. T., Lamarque, J.-F., Matsumoto, K., Montzka, S., Raper, S., Riahi, K., Thomson, A. M., Velders, G. J. M., and van Vuuren, D. P.: The RCP greenhouse gas concentrations and their extensions from 1765 to 2300, Climatic Change, 109, 213–241, doi:10.1007/s10584-011-0156-z, 2011.

495 Morgenstern, O., Braesicke, P., O'Connor, F. M., Bushell, A. C., Johnson, C. E., Osprey, S. M., and Pyle, J. A.: Evaluation of the new UKCA climate-composition model – Part 1: The stratosphere, Geosci. Model Dev., 2, 43–57, doi:10.5194/gmd-2-43-2009, 2009.

Morgenstern, O., Akiyoshi, H., Bekki, S., Braesicke, P., Butchart, N., Chipperfield, M. P., Cugnet, D., Deushi, M., Dhomse, S. S., Garcia, R. R., Gettelman, A., Gillett, N. P., Hardiman, S. C., Jumelet, J., Kinnison, D. E.,

500   Lamarque, J.-F., Lott, F., Marchand, M., Michou, M., Nakamura, T., Olivié, D., Peter, T., Plummer, D., Pyle, J. A., Rozanov, E., Saint-Martin, D., Scinocca, J. F., Shibata, K., Sigmond, M., Smale, D., Teyssèdre, H., Tian, W., Voldoire, A., and Yamashita, Y.: Anthropogenic forcing of the Northern Annular Mode in CCMVal-2 models, J. Geophys. Res. Atmos., 115, D00M03, doi:10.1029/2009JD013347, 2010.

Morgenstern, O., Zeng, G., Abraham, N. L., Telford, P. J., Braesicke, P., Pyle, J. A., Hardiman, S. C.,

505   O'Connor, F. M., and Johnson, C. E.: Impacts of climate change, ozone recovery, and increasing methane on surface ozone and the tropospheric oxidizing capacity, J. Geophys. Res. Atmos., 118, 1028–1041, doi:10.1029/2012JD018382, 2013.

Morgenstern, O., Hegglin, M. I., Rozanov, E., O'Connor, F. M., Abraham, N. L., Akiyoshi, H., Archibald, A. T., Bekki, S., Butchart, N., Chipperfield, M. P., Deushi, M., Dhomse, S. S., Garcia, R. R., Hardiman, S. C.,

510   Horowitz, L. W., Jöckel, P., Josse, B., Kinnison, D., Lin, M. Y., Mancini, E., Manyin, M. E., Marchand, M., Marécal, V., Michou, M., Oman, L. D., Pitari, G., Plummer, D. A., Revell, L. E., Saint-Martin, D., Schofield, R., Stenke, A., Stone, K., Sudo, K., Tanaka, T. Y., Tilmes, S., Yamashita, S., Yoshida, Y., and Zeng, G.:

Review of the global models used within phase 1 of the Chemistry-Climate Model Initiative (CCMI), Geosci. Model Dev., 10, 639–671, doi:10.5194/gmd-10-639-2017, 2017.

515 Naik, V., Voulgarakis, A., Fiore, A. M., Horowitz, L. W., Lamarque, J.-F., Lin, M., Prather, M. J., Young, P. J., Bergmann, D., Cameron-Smith, P. J., Cionni, I., Collins, W. J., Dalsøren, S. B., Doherty, R., Eyring, V., Faluvegi, G., Folberth, G. A., Josse, B., Lee, Y. H., MacKenzie, I. A., Nagashima, T., van Noije, T. P. C., Plummer, D. A., Righi, M., Rumbold, S. T., Skeie, R., Shindell, D. T., Stevenson, D. S., Strode, S., Sudo, K., Szopa, S., and Zeng, G.: Preindustrial to present–day changes in tropospheric hydroxyl radical and methane

520 lifetime from the Atmospheric Chemistry and Climate Model Intercomparison Project (ACCMIP), Atmos. Chem. Phys., 13, 5277–5298, doi:10.5194/acp-13-5277-2013, 2013.

Newman, P. A., Daniel, J. S., Waugh, D. W., and Nash, E. R.: A new formulation of equivalent effective stratospheric chlorine (EESC), Atmos. Chem. Phys., 7, 4537–4552, doi:10.5194/acp-7-4537-2007, 2007.

Oberländer-Hayn, S., Gerber, E. P., Abalichin, J., Akiyoshi, H., Kerschbaumer, A., Kubin, A., Kunze, M.,

525 Langematz, U., Meul, S., Michou, M., Morgenstern, O., and Oman, L. D.: Is the Brewer-Dobson circulation increasing or moving upward?, Geophys. Res. Lett., 43, 1772–1779, doi:10.1002/2015GL067545, 2016.

Oman, L. D., Douglass, A. R., Salawitch, R. J., Canty, T. P., Ziemke, J. R., and Manyin, M.: The effect of representing bromine from VSLS on the simulation and evolution of Antarctic ozone, Geophys. Res. Lett., 43, 9869–9876, doi:10.1002/2016GL070471, 2016.

530 Pitari, G., Aquila, V., Kravitz, B., Robock, A., Watanabe, S., Cionni, I., De Luca, N., Di Genova, G., Mancini, E., and Tilmes, S.: Stratospheric ozone response to sulfate geoengineering: Results from the Geoengineering Model Intercomparison Project (GeoMIP), J. Geophys. Res. Atmos., 119, 2629–2653, doi:10.1002_2013JD020566, 2014.

Portmann, R. W., Daniel, J. S., and Ravishankara, A. R.: Stratospheric ozone depletion due to nitrous oxide: in-

535 fluences of other gases, Phil. Trans. Royal Soc. B: Biolog. Sci., 367, 1256–1264, doi:10.1098/rstb.2011.0377, 2012.

Prather, M., Ehhalt, D., Dentener, F., Derwent, R., Dlugokencky, E., Holland, E., Isaksen, I., Katima, J., Kirchhoff, V., Matson, P., Midgley, P., and Wang, M.: Atmospheric Chemistry and Greenhouse Gases, in: Climate Change 2001: The Scientific Basis. Third Assessment Report of the Intergovernmental Panel on Climate

540 Change, edited by Houghton, J., Ding, Y., Griggs, D., Noguer, M., van der Linden, P., Dai, X., Maskell, K., and Johnson, C., Cambridge University Press, Cambridge, UK, 2001.

Ravishankara, A. R., Daniel, J. S., and Portmann, R. W.: Nitrous oxide (N_2O): the dominant ozone-depleting substance emitted in the 21st century, Science, 326, 123–125, doi:10.1126/science.1176985, 2009.

Revell, L. E., Bodeker, G. E., Huck, P. E., Williamson, B. E., and Rozanov, E.: The sensitivity of strato-

545 spheric ozone changes through the 21st century to N_2O and CH_4, Atmos. Chem. Phys., 12, 11 309–11 317, doi:10.5194/acp-12-11309-2012, 2012a.

Revell, L. E., Bodeker, G. E., Smale, D., Lehmann, R., Huck, P. E., Williamson, B. E., Rozanov, E., and Struthers, H.: The effectiveness of N_2O in depleting stratospheric ozone, Geophys. Res. Lett., 39, doi:10.1029/2012GL052143, l15806, 2012b.

550 Revell, L. E., Tummon, F., Stenke, A., Sukhodolov, T., Coulon, A., Rozanov, E., Garny, H., Grewe, V., and Peter, T.: Drivers of the tropospheric ozone budget throughout the 21st century under the medium-high climate scenario RCP 6.0, Atmos. Chem. Phys., 15, 5887–5902, doi:10.5194/acp-15-5887-2015, 2015.

Riahi, K., van Vuuren, D. P., Kriegler, E., Edmonds, J., O'Neill, B. C., Fujimori, S., Bauer, N., Calvin, K., Dellink, R., Fricko, O., Lutz, W., Popp, A., Cuaresma, J. C., KC, S., Leimbach, M., Jiang, L., Kram, T., Rao, S., Emmerling, J., Ebi, K., Hasegawa, T., Havlik, P., Humpenöder, F., Da Silva, L. A., Smith, S., Stehfest, E., Bosetti, V., Eom, J., Gernaat, D., Masui, T., Rogelj, J., Strefler, J., Drouet, L., Krey, V., Luderer, G., Harmsen, M., Takahashi, K., Baumstark, L., Doelman, J., Kainuma, M., Klimont, Z., Marangoni, G., Lotze-Campen, H., Obersteiner, M., Tabeau, A., and Tavoni, M.: The Shared Socioeconomic Pathways and their energy, land use, and greenhouse gas emissions implications: an overview, Global Environ. Change, 42, 153–168, doi:10.1016/j.gloenvcha.2016.05.009, 2016.

Scinocca, J. F., McFarlane, N. A., Lazare, M., Li, J., and Plummer, D.: Technical Note: The CCCma third generation AGCM and its extension into the middle atmosphere, Atmos. Chem. Phys., 8, 7055–7074, doi:10.5194/acp-8-7055-2008, 2008.

Solomon, S.: Stratospheric ozone depletion: A review of concepts and history, Rev. Geophys., 37, 275–316, doi:10.1029/1999RG900008, 1999.

Solomon, S., Ivy, D. J., Kinnison, D., Mills, M. J., Neely, R. R., and Schmidt, A.: Emergence of healing in the Antarctic ozone layer, Science, 353, 269–274, doi:10.1126/science.aae0061, 2016.

Stenke, A., Schraner, M., Rozanov, E., Egorova, T., Luo, B., and Peter, T.: The SOCOL version 3.0 chemistry–climate model: description, evaluation, and implications from an advanced transport algorithm, Geosci. Model Dev., 6, 1407–1427, doi:10.5194/gmd-6-1407-2013, 2013.

Stevenson, D., Johnson, C., Collins, W., Derwent, R., and Edwards, J.: Future estimates of tropospheric ozone radiative forcing and methane turnover – the impact of climate change, Geophys. Res. Lett., 27, 2073–2076, 2000.

Stolarski, R. S., Douglass, A. R., Oman, L. D., and Waugh, D. W.: Impact of future nitrous oxide and carbon dioxide emissions on the stratospheric ozone layer, Environ. Res. Lett., 10, 034 011, http://stacks.iop.org/1748-9326/10/i=3/a=034011, 2015.

Thompson, D. W. J., Solomon, S., Kushner, P. J., England, M. H., Grise, K. M., and Karoly, D. J.: Signatures of the Antarctic ozone hole in Southern Hemisphere surface climate change, Nature Geosci., 4, 741–749, 2011.

Tian, W. and Chipperfield, M. P.: A new coupled chemistry-climate model for the stratosphere: The importance of coupling for future O_3 – climate predictions, Q. J. Roy. Meteor. Soc., 131, 281–303, 2005.

Voulgarakis, A., Naik, V., Lamarque, J.-F., Shindell, D. T., Young, P. J., Prather, M. J., Wild, O., Field, R. D., Bergmann, D., Cameron-Smith, P., Cionni, I., Collins, W. J., Dalsøren, S. B., Doherty, R. M., Eyring, V., Faluvegi, G., Folberth, G. A., Horowitz, L. W., Josse, B., MacKenzie, I. A., Nagashima, T., Plummer, D. A., Righi, M., Rumbold, S. T., Stevenson, D. S., Strode, S. A., Sudo, K., Szopa, S., and Zeng, G.: Analysis of present day and future OH and methane lifetime in the ACCMIP simulations, Atmos. Chem. Phys., 13, 2563–2587, doi:10.5194/acp-13-2563-2013, 2013.

Voulgarakis, A., Savage, N. H., Wild, O., Carver, G. D., Clemitshaw, K. C., and Pyle, J. A.: Upgrading photolysis in the p–TOMCAT CTM: model evaluation and assessment of the role of clouds, Geosci. Model Dev., 2, 59–72, 2009.

WMO: Scientific Assessment of Ozone Depletion: 2014, vol. 55 of *Global Ozone Research and Monitoring Project*, World Meteorological Organization, 416pp, 2014.

Young, P. J., Archibald, A. T., Bowman, K. W., Lamarque, J.-F., Naik, V., Stevenson, D. S., Tilmes, S., Voulgarakis, A., Wild, O., Bergmann, D., Cameron-Smith, P., Cionni, I., Collins, W. J., Dalsøren, S. B., Doherty, R. M., Eyring, V., Faluvegi, G., Horowitz, L. W., Josse, B., Lee, Y. H., MacKenzie, I. A., Nagashima, T., Plummer, D. A., Righi, M., Rumbold, S. T., Skeie, R. B., Shindell, D. T., Strode, S. A., Sudo, K., Szopa, S., and Zeng, G.: Pre-industrial to end 21st century projections of tropospheric ozone from the Atmospheric Chemistry and Climate Model Intercomparison Project (ACCMIP), Atmos. Chem. Phys., 13, 2063–2090, doi:10.5194/acp-13-2063-2013, 2013.
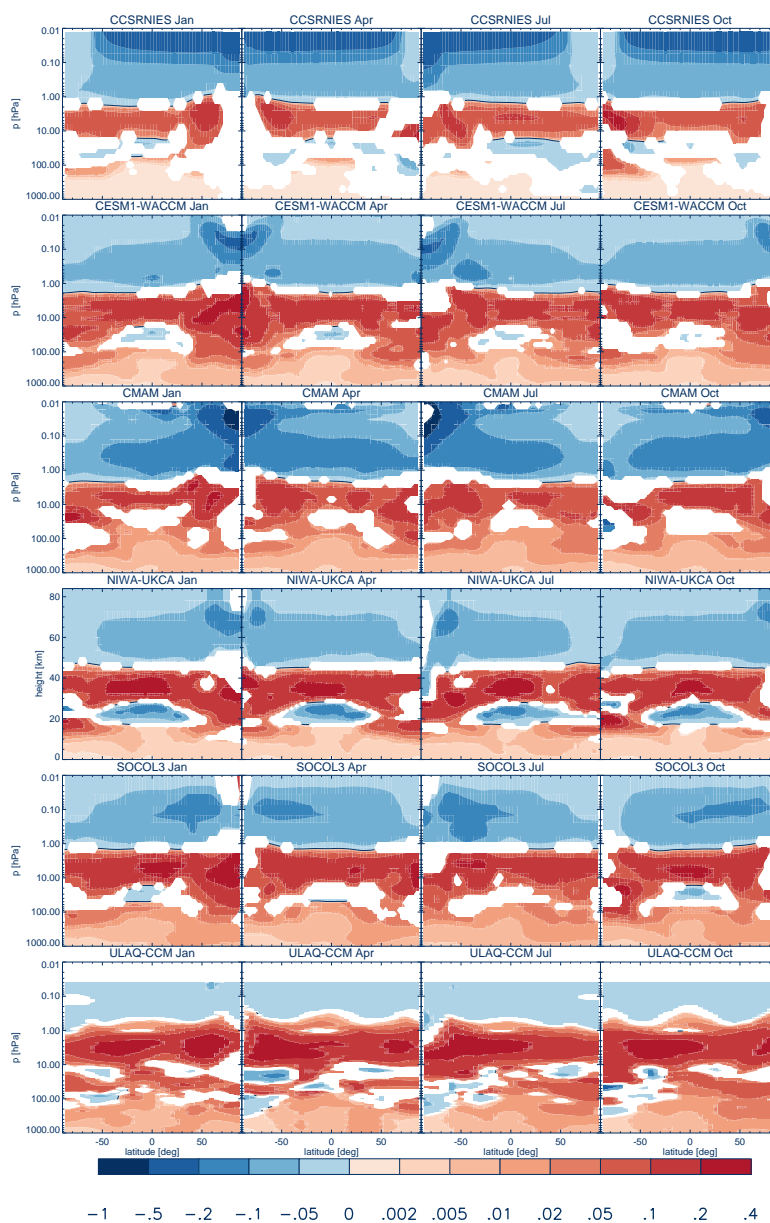
Figure 1: Ratio of zonal-mean ozone volume mixing ratio changes to VMR changes in surface CH_4 (a) as derived from the REF-C2 and SEN-C2-fCH4 simulations. a is dimensionless. The colour white indicates that a is not significantly different from 0 at the 95% confidence interval. The plots for ULAQ-CCM (bottom row) have no data above 0.04 hPa.
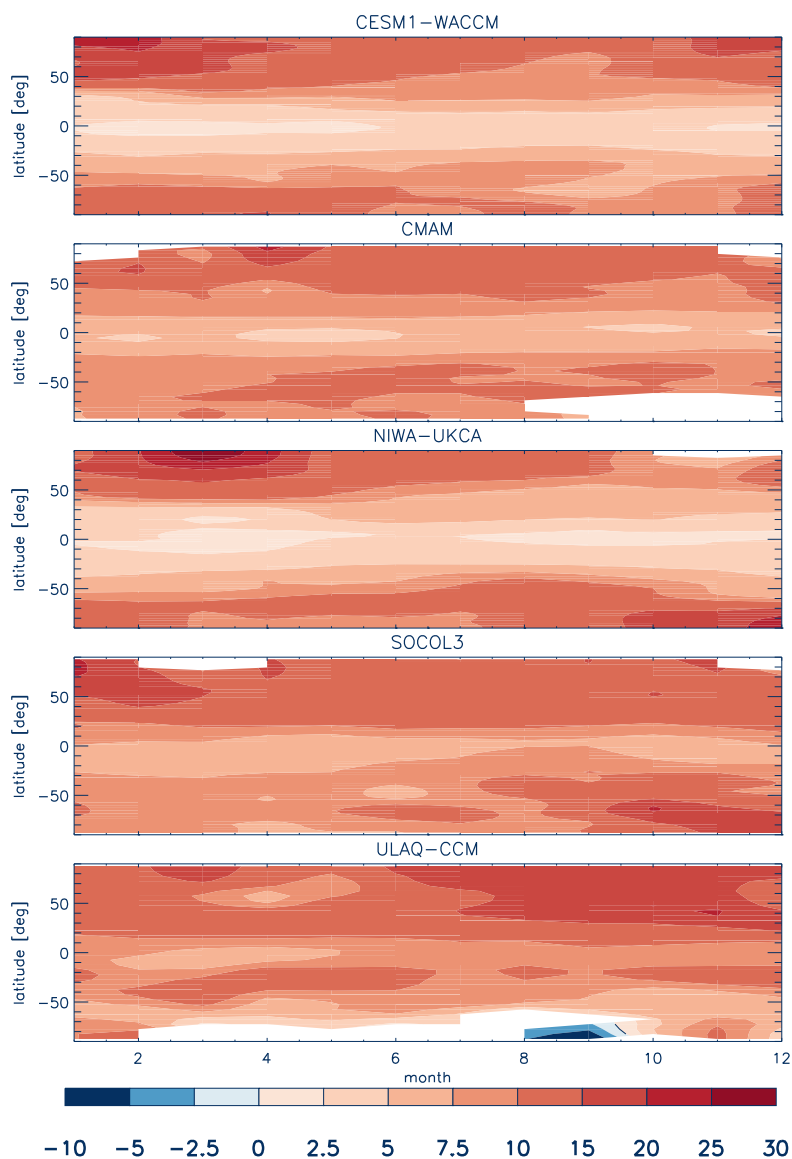
Figure 2: Ratio of zonal-mean total-column ozone changes to VMR changes in surface CH_4 (in Dobson Units / ppmv) as derived from the REF-C2 and SEN-C2-fCH4 simulations. The colour white indicates insignificantly differences from 0 at the 95% confidence interval.
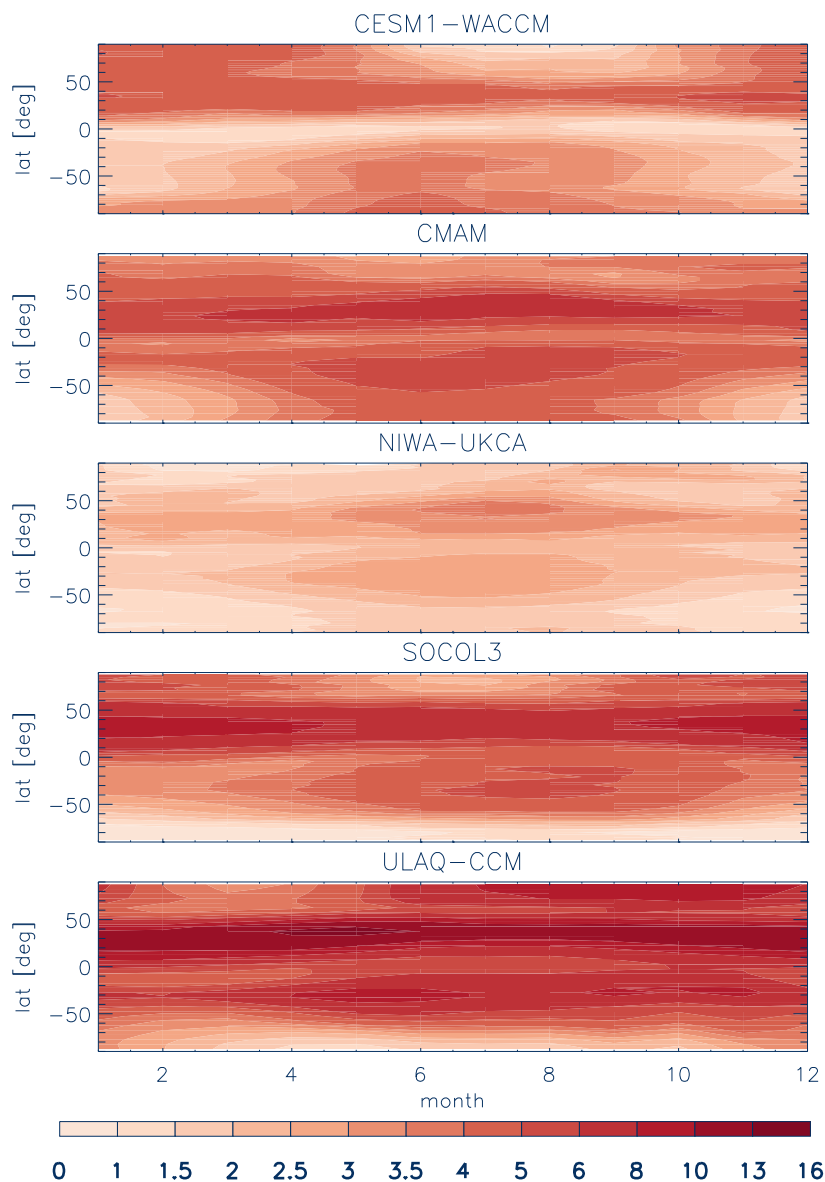
Figure 3: Ratio of zonal-mean surface ozone changes to to changes in surface CH_4 (in ppbv / ppmv) as derived from the REF-C2 and SEN-C2-fCH4 simulations. The colour white indicates insignificantly differences from 0 at the 95% confidence interval.
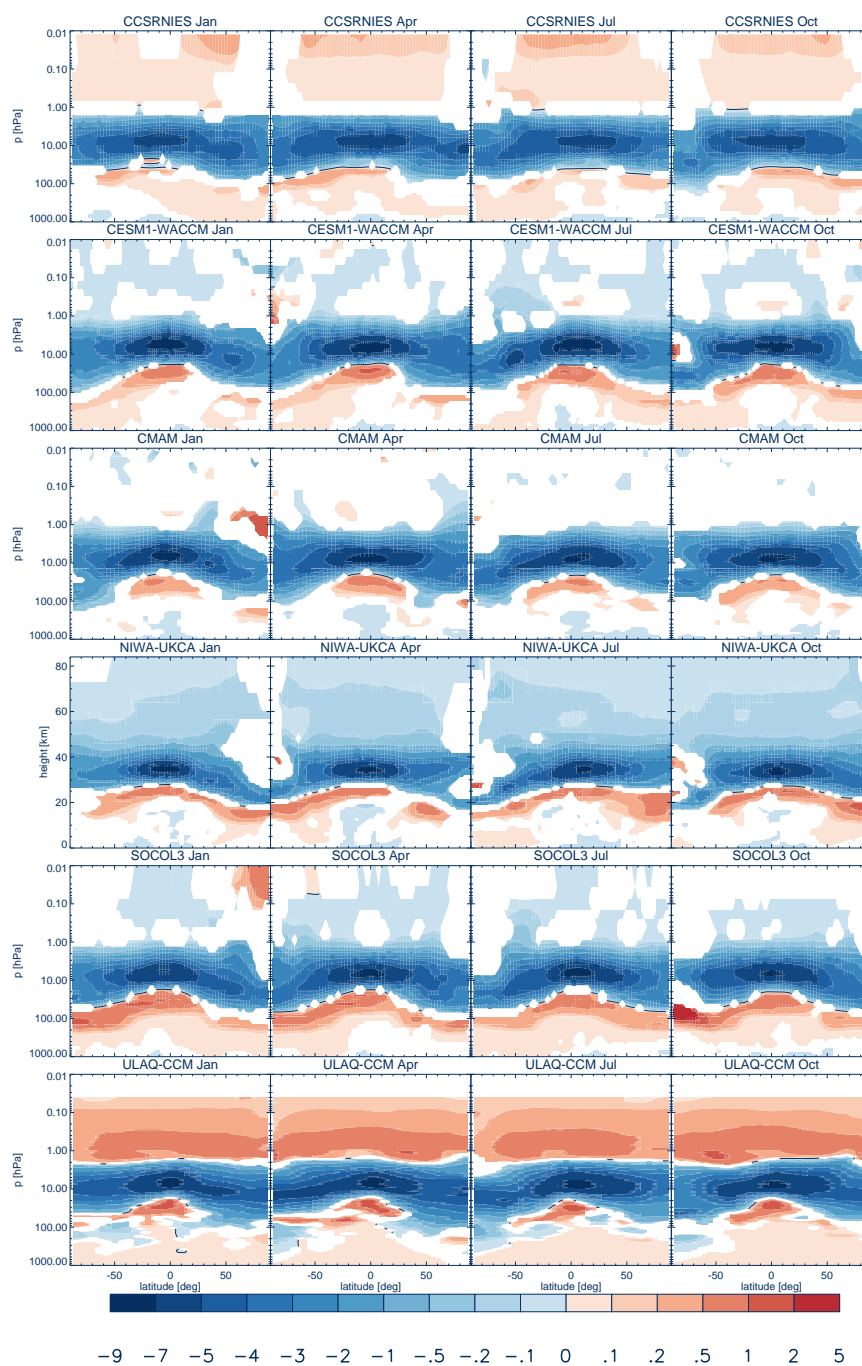
Figure 4: Same as figure 1 but for N_2O.
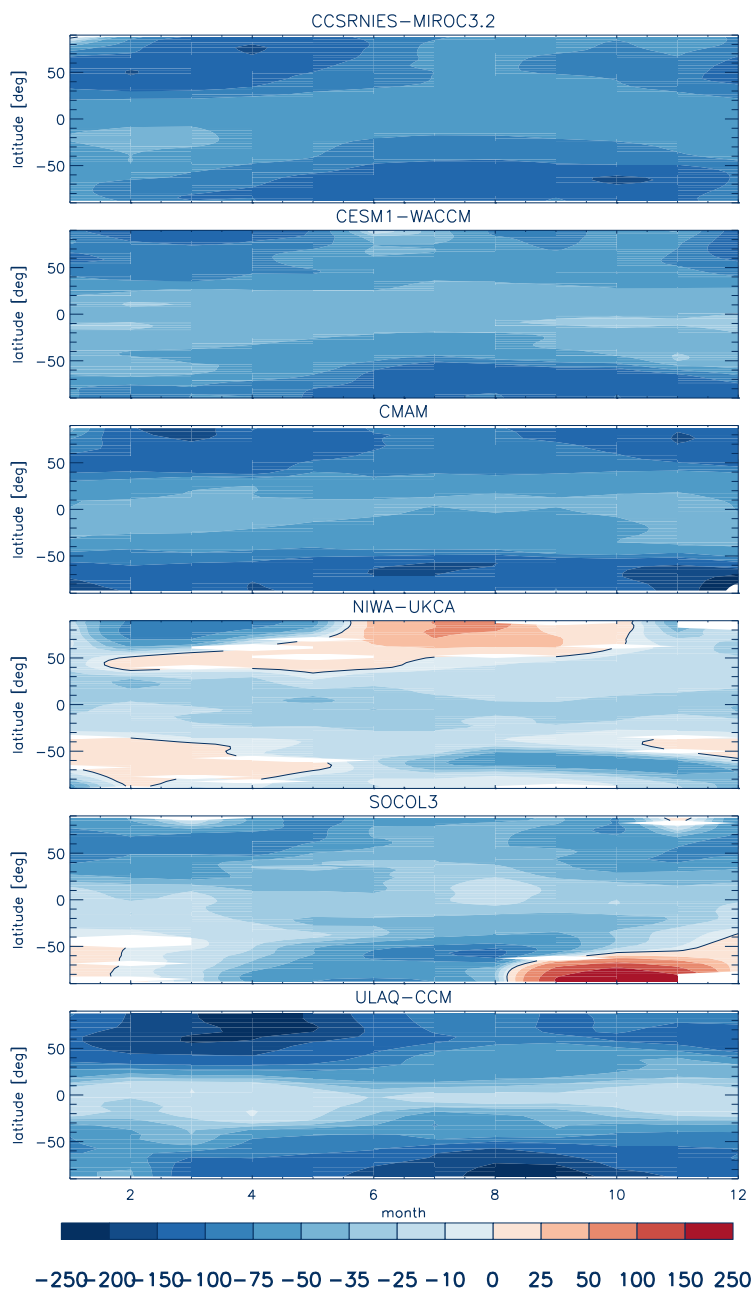
Figure 5: Same as figure 2 but for N_2O, in units of DU/ppmv, derived from the REF-C2 and SEN-C2-fN2O simulations.
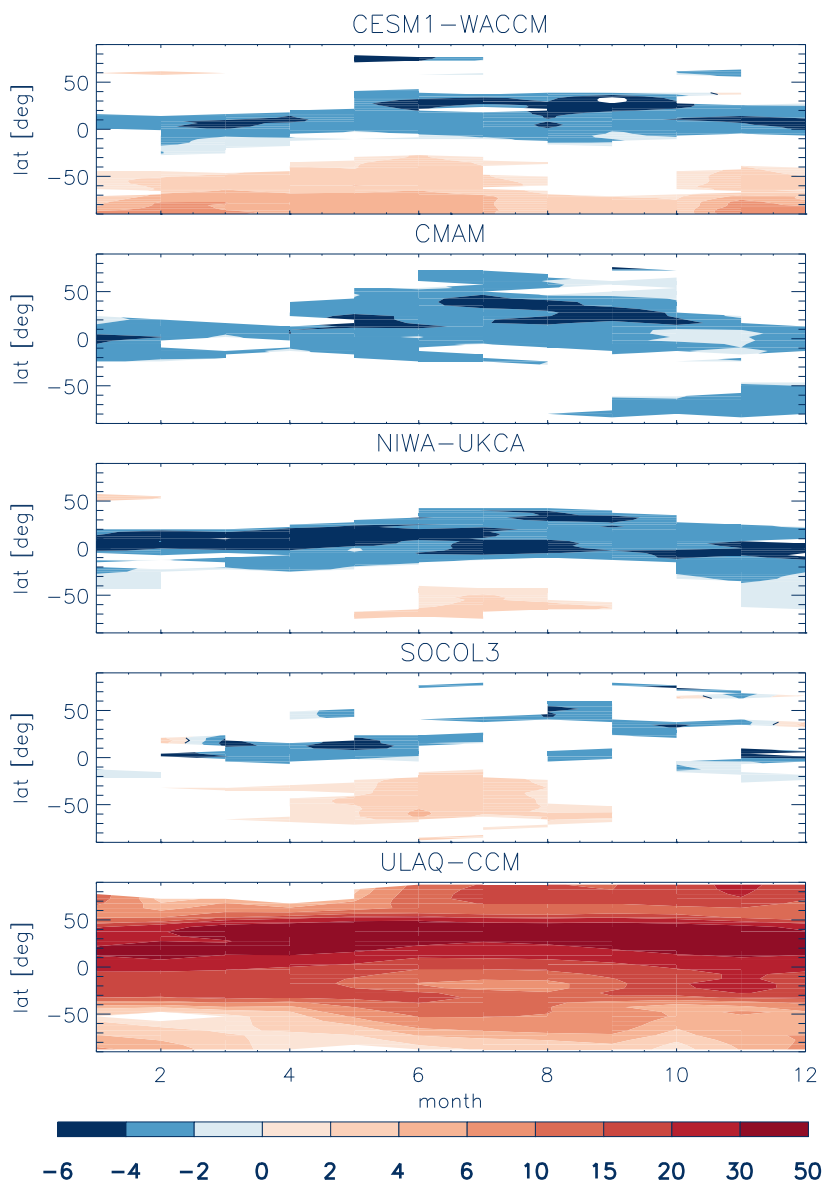
Figure 6: Same as figure 3 but for N$_2$O, in ppbv/ppmv, as derived from the REF-C2 and SEN-C2-fN2O simulations.
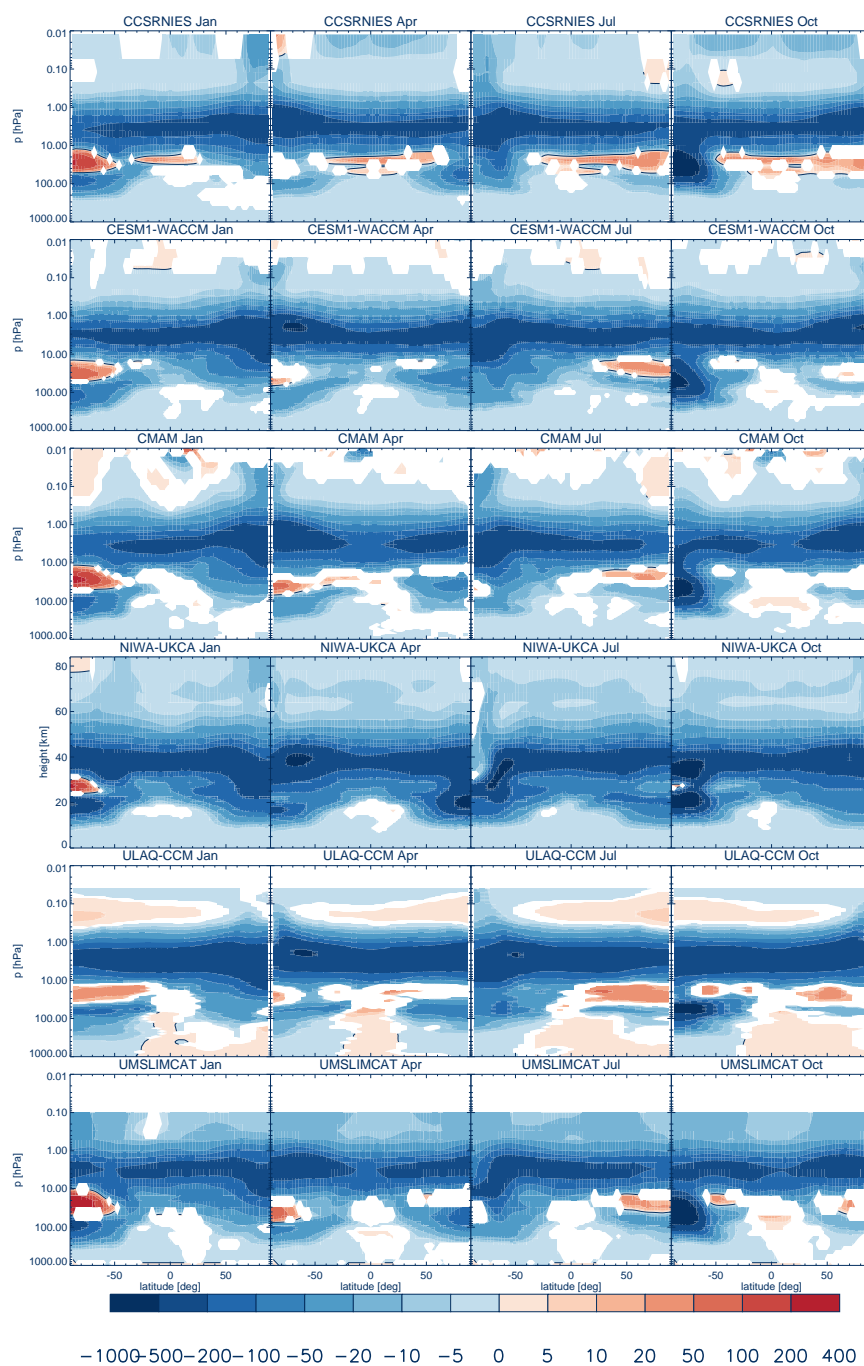
Figure 7: Same as figure 1 but for Cl_y.
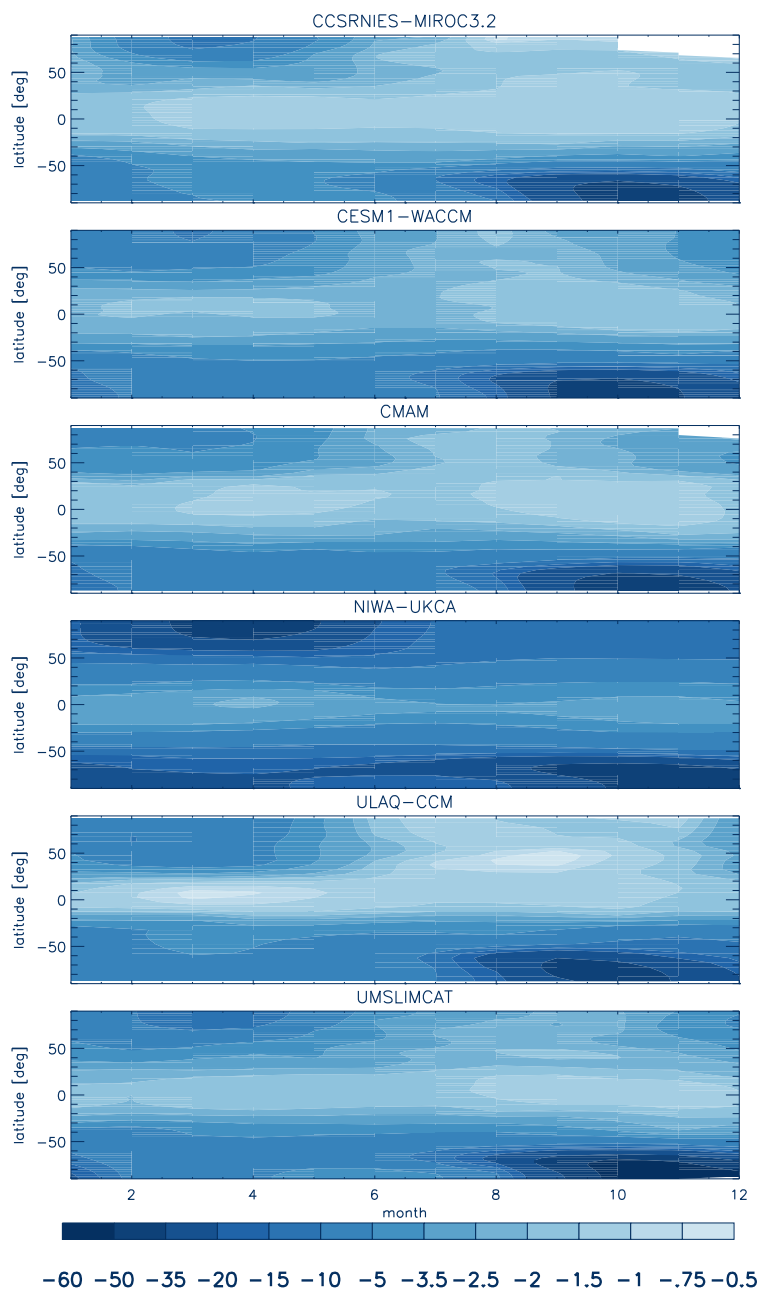
Figure 8: Same as figure 2 but for Cl_y, in units of DU/ppbv (Cl^{eq}), derived from the REF-C2 and SEN-C2-fODS simulations.
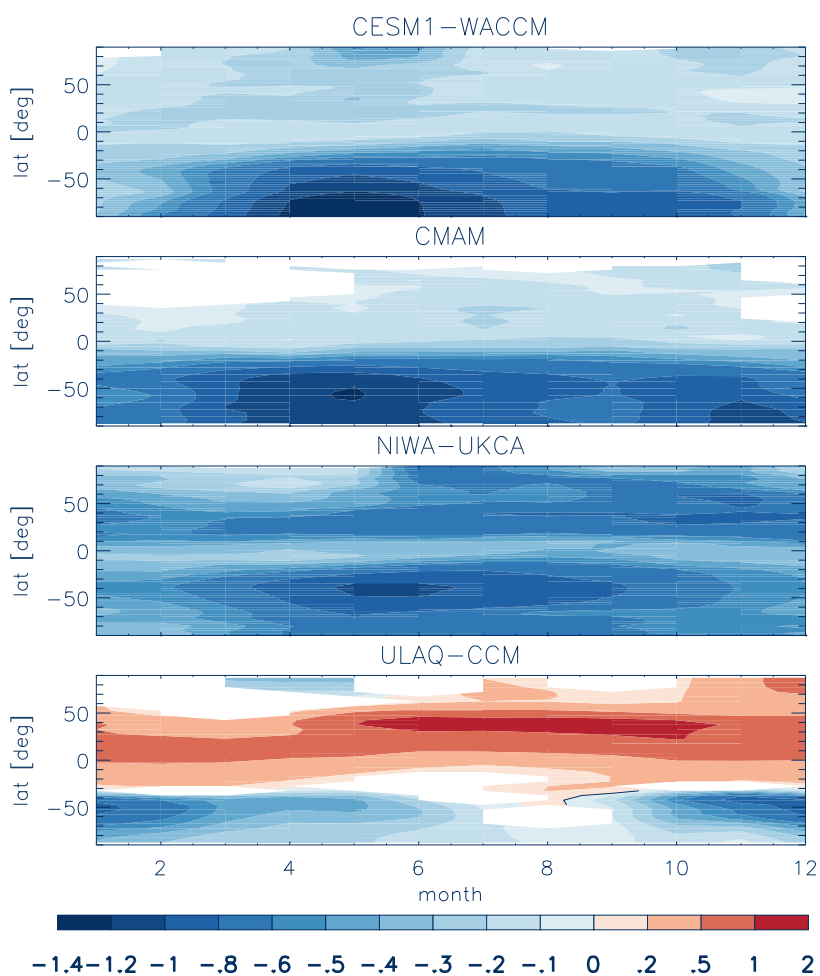
Figure 9: Ratio of zonal-mean surface ozone changes to to changes in surface Cl^{eq} (in ppbv / ppbv) as derived from the REF-C2 and SEN-C2-fODS simulations.
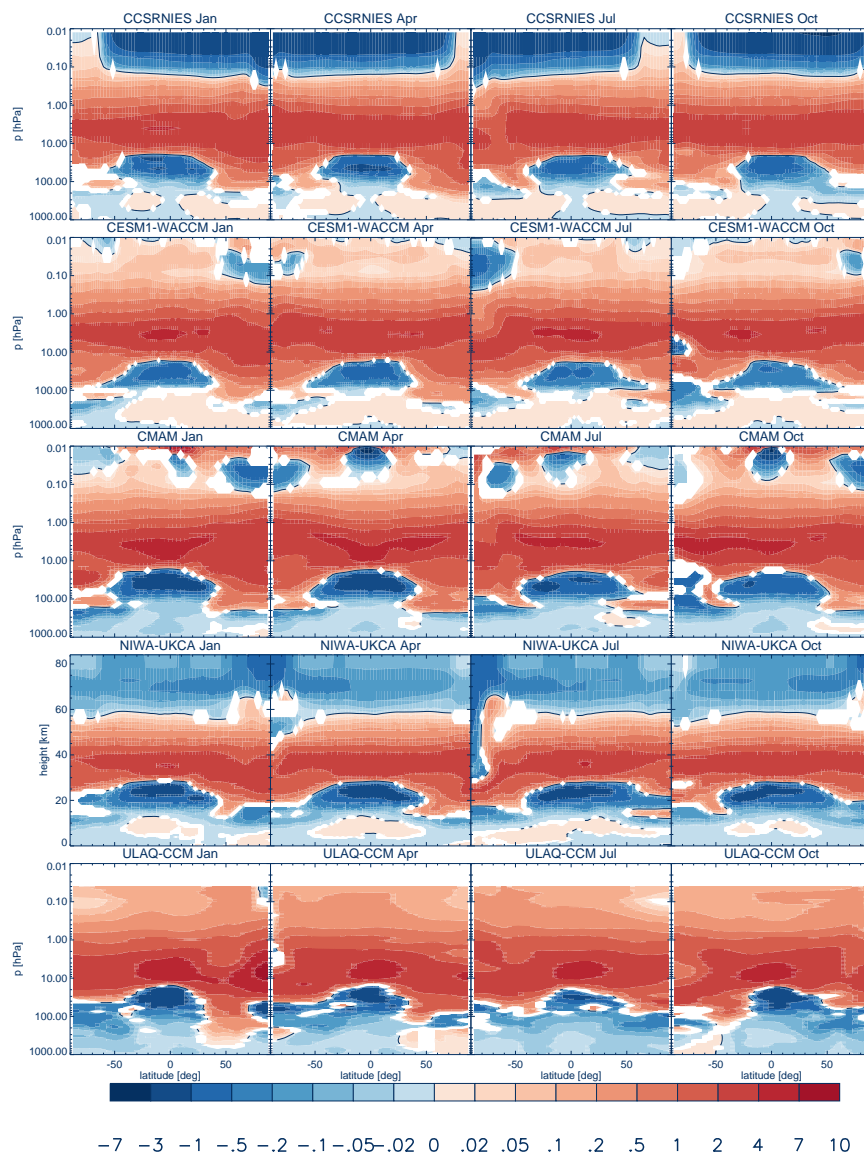
Figure 10: Same as figure 1 but for CO_2^{eq}. Here units are 10^{-3} ppmv/ppmv.
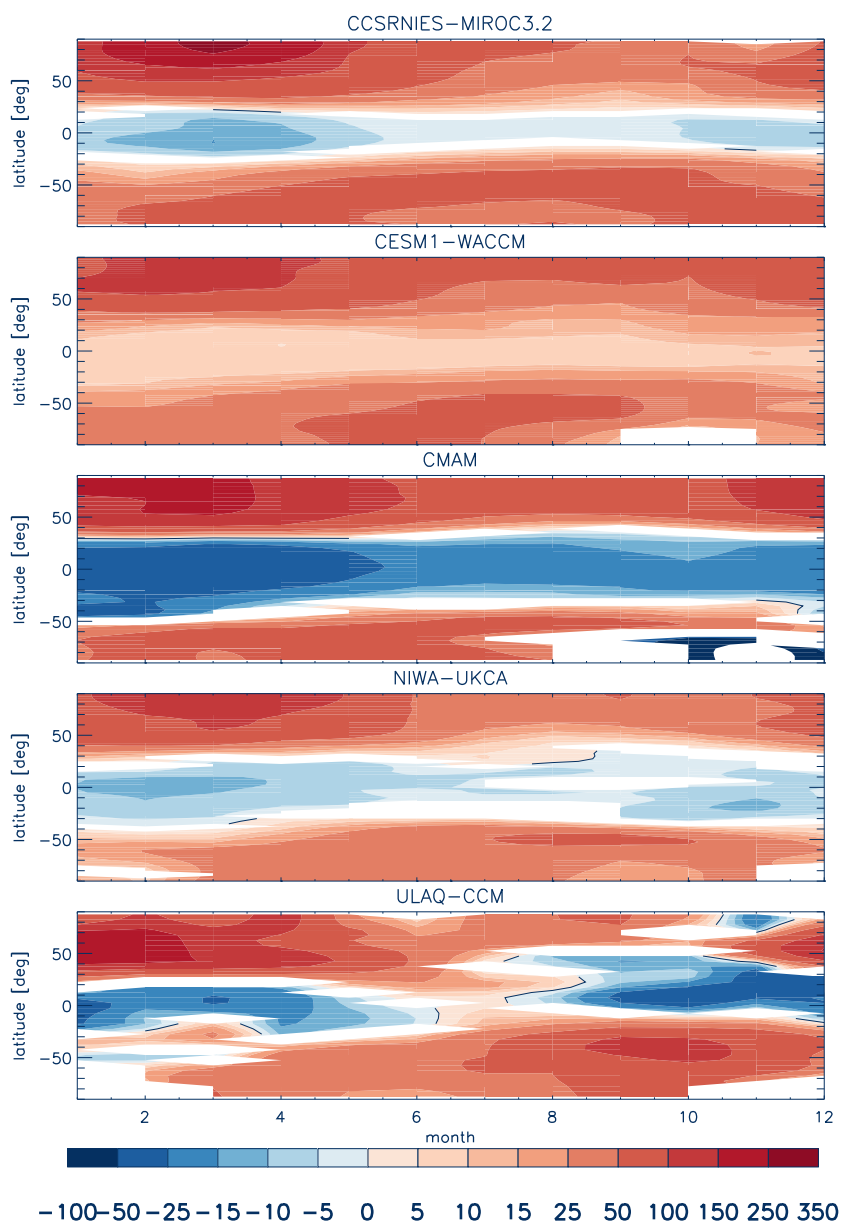
Figure 11: Same as figure 2 but for CO_2^{eq}, in units of 10^{-3} DU/ppmv (CO_2^{eq}), derived from the REF-C2, SEN-C2-fGHG, SEN-C2-fCH4, and SEN-C2-fN2O simulations.
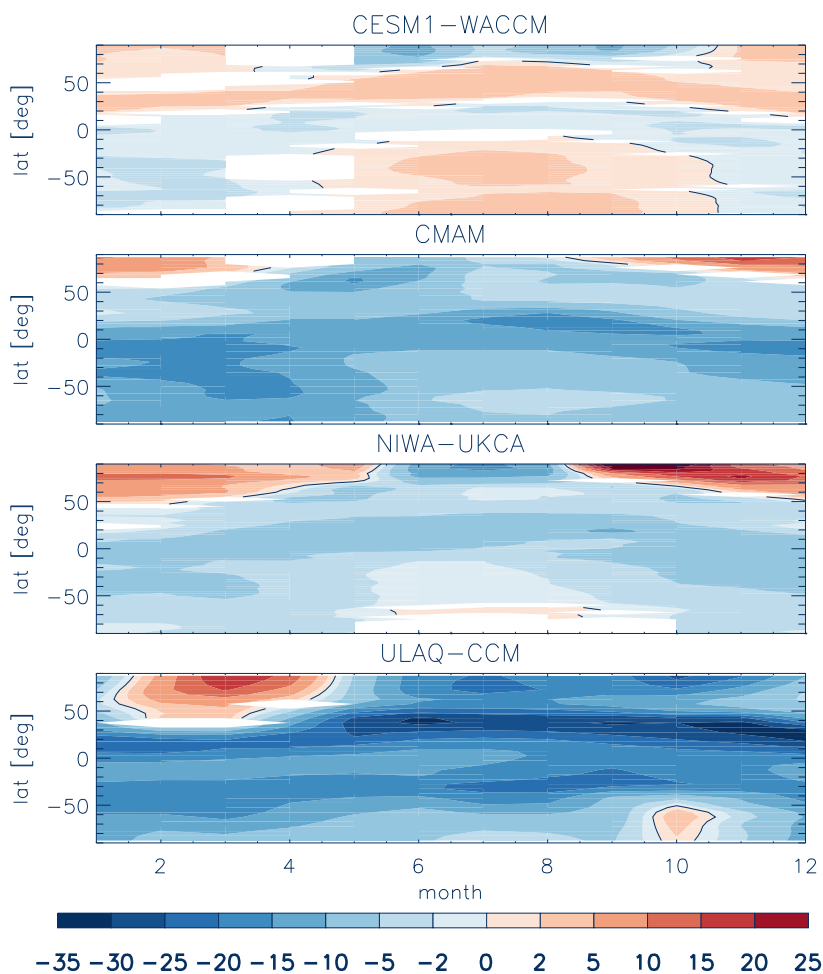
Figure 12: Ratio of zonal-mean surface ozone changes to changes in surface CO_2^{eq}, times 10^6, as derived from the REF-C2, SEN-C2-fGHG, SEN-C2-fCH4, and SEN-C2-fN2O.
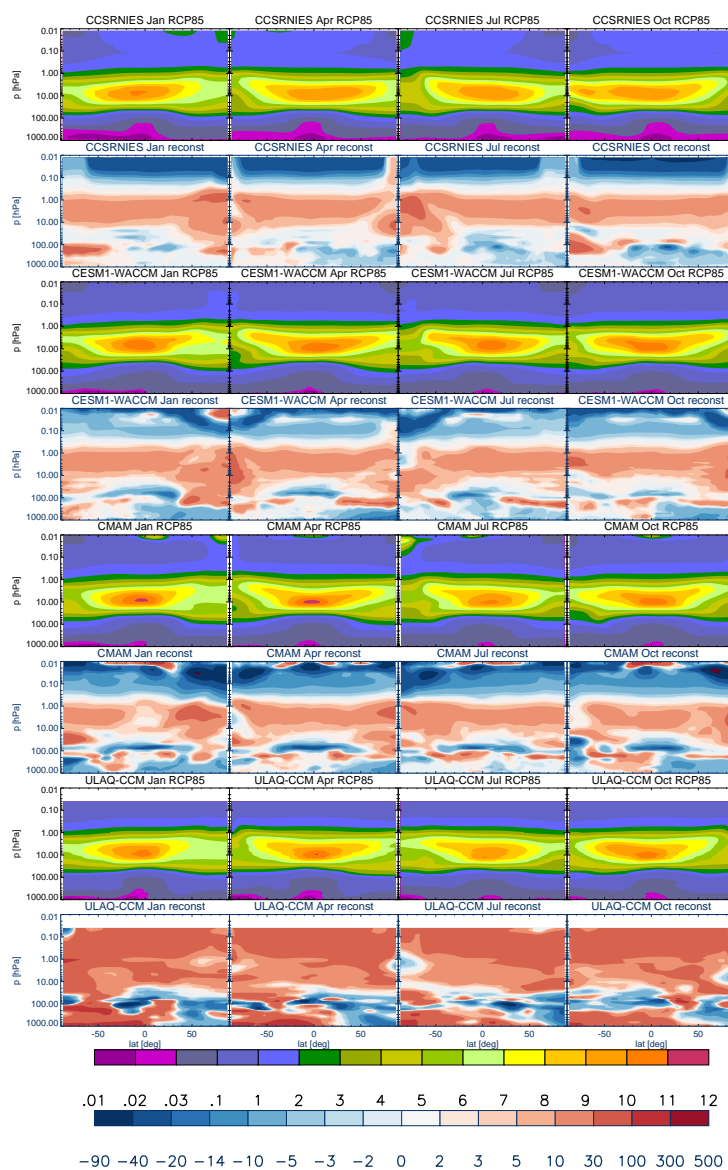
Figure 13: Rows 1, 3, 5, and 7: Zonal-mean ozone (ppmv), averaged individually for the months of January, April, July, and October, for the years 2090-2099 of the RCP 8.5 scenario, as simulated by the CCSRNIES-MIROC3.2, CESM1-WACCM, CMAM, and ULAQ-CCM models. Rows 2,4,6, and 8: Percentage difference between the rescaled and simulated ozone fields. The rescaling is based on the REF-C2 simulations and the a, b, and d coefficients as derived versus the SEN-C2-fCH4, -fN2O, and -fGHG simulations. Note that the ODSs evolve identically in REF-C2 and in SEN-C2-RCP85.